

Supporting Information

“Heteronuclear DNP of Protons and Deuterons with TEMPOL”

Kaminker I.^{+a}, Shimon D.⁺, Hovav Y.^b, Feintuch A., and Vega S.*

Weizmann institute of Science, Rehovot , Israel

^a present address: Department of Chemistry and Biochemistry, University of California, Santa Barbara, U.S.A.

^b present address: Department of Applied Physics, Hebrew University of Jerusalem, Israel

In this work all the ¹H-DNP and ²H-DNP experiments were preceded with presaturation on the nuclei in the system. Experiments with ¹H detection were preceded with a saturation pulse train at the ¹H frequency. Experiments with ²H detection were preceded by saturation trains at both ¹H and ²H NMR frequencies. The parameters of the saturation trains employed at different NMR probes are detailed in Table S1. The saturation train was composed of pairs of pulses with alternating x and y phases, with a delay between them, repeated many times. The total length of the saturation train can be calculated as follows: $2x[(\text{pulse length}) + (\text{delay length})]x(\text{number of repeats})$.

In this work two probes were employed, one for ¹H detection using a previously described probe [1], and a second for ²H detection using a new probe built with tuning and matching capacitors positioned in close proximity to the NMR coil. Each probe was used for detecting the appropriate nucleus, and also for saturating both nuclei. For example, if using the ²H probe, the power on the ²H channel was ~ 60 kHz, and so it was possible to saturate the ²H nucleus in 60 pulse pairs, while the power using for saturating the ¹H nuclei was ~ 10 kHz and so 600 pulse pairs were needed. More information about the tuning of each probe to two nuclear frequencies can be found in the main text.

| Probe | Nuclei | Pulse length (μs) | Delay length (μs) | Number of Repeats | ω_1 (kHz) |
|----------------------|---|--------------------------------|--------------------------------|-------------------|------------------|
| ¹ H probe | ¹ H (saturation + detection) | 4 | 50 | 60 | ~ 100 |
| | ² H(saturation) | 10 | 50 | 600 | ~ 10 |
| ² H probe | ¹ H (saturation) | 10 | 50 | 600 | ~ 10 |
| | ² H(saturation + detection) | 2 | 50 | 60 | ~ 60 |

Table. S1: Saturation pulse train parameters used in 2H and 1H DNP experiments.

First we show that the ^1H -DNP spectrum of the “ H_2O ” sample at 6 K does not change its shape as a function of t_{excite} . As can be seen in Fig. S1 both after $t_{excite} = 1$ sec and 120 sec the shapes are exactly the same.

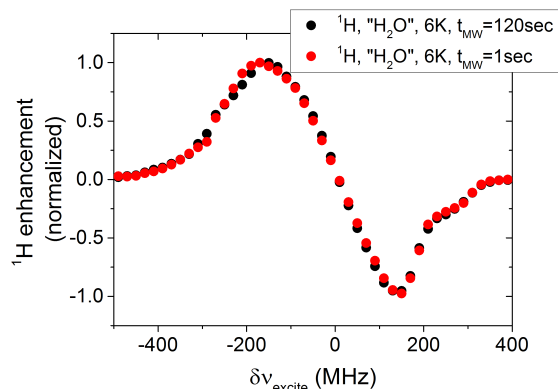


Figure. S1: Normalized DNP spectra of the ^1H nuclei at 6 K measured at different values of t_{excite} . The steady state DNP spectrum is plotted in black, and the spectrum with a short t_{excite} in red, to allow comparison of the spectra. The x-axis is plotted with reference to $\nu_{ref} = 95$ GHz.

In order to fit the DNP spectra of the “ H_2O ” sample at 6 K and at 20 K, ELDOR spectra were measured and fitted. The ELDOR spectra at different detection frequencies at 6 K are shown in Fig. S2 and the ELDOR spectra at 20 K in Fig. S3. The figures also include the fits. The fitting parameters are listed in the main text.

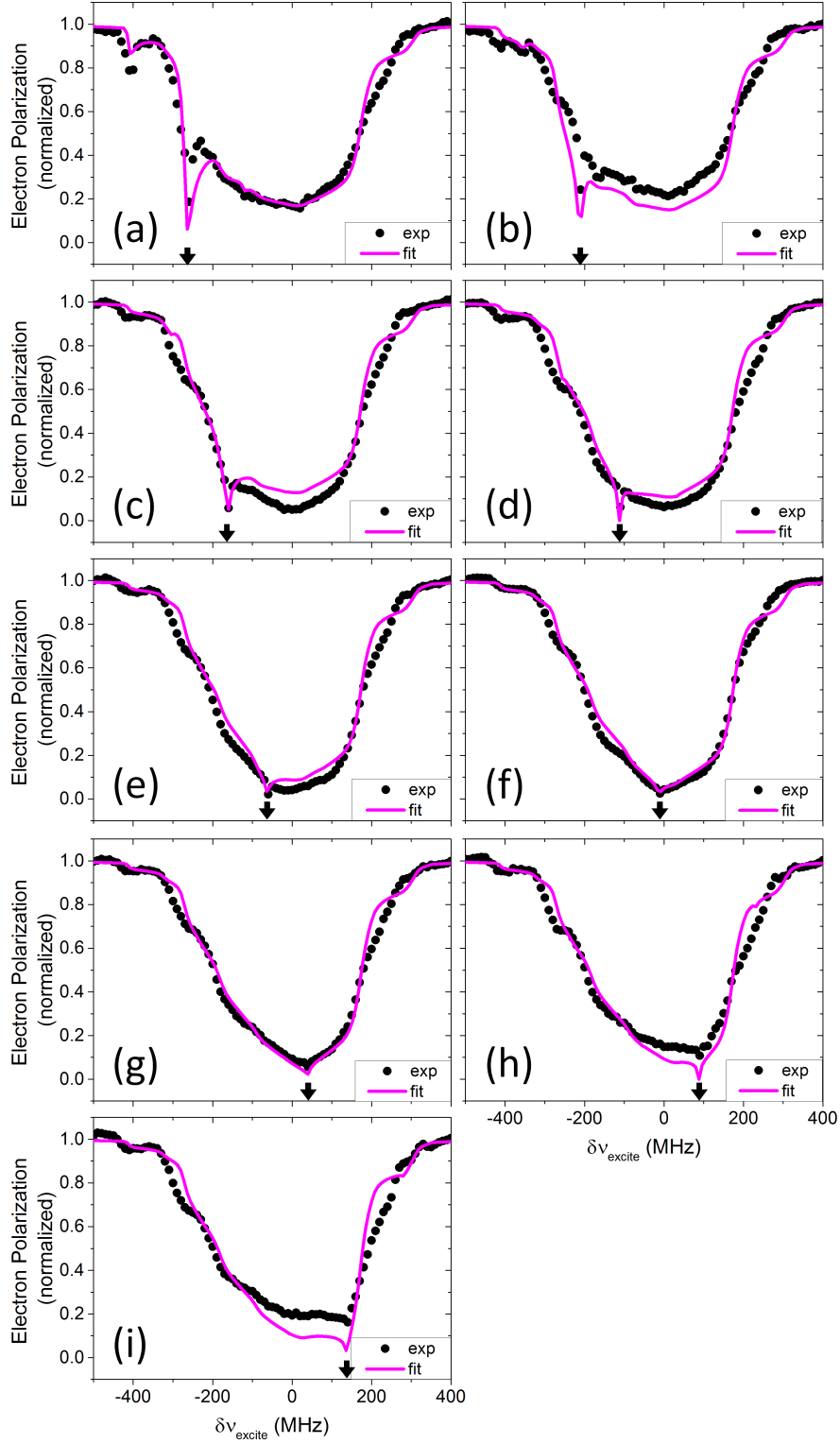


Figure. S2: Experimental ELDOR spectra measured at 6 K on the “H₂O” sample (black symbols) overlaid with the simulated ELDOR spectra (magenta lines). The detection frequencies are marked by the small black arrows: (a) $\delta\nu_{detect} = -260$ MHz, (b) $\delta\nu_{detect} = -210$ MHz, (c) $\delta\nu_{detect} = -160$ MHz, (d) $\delta\nu_{detect} = -110$ MHz, (e) $\delta\nu_{detect} = -60$ MHz, (f) $\delta\nu_{detect} = -1$ MHz, (g) $\delta\nu_{detect} = 40$ MHz, (h) $\delta\nu_{detect} = 1$ MHz and (i) $\delta\nu_{detect} = 140$ MHz. The x-axis is plotted with reference to $\nu_{ref} = 95$ GHz.

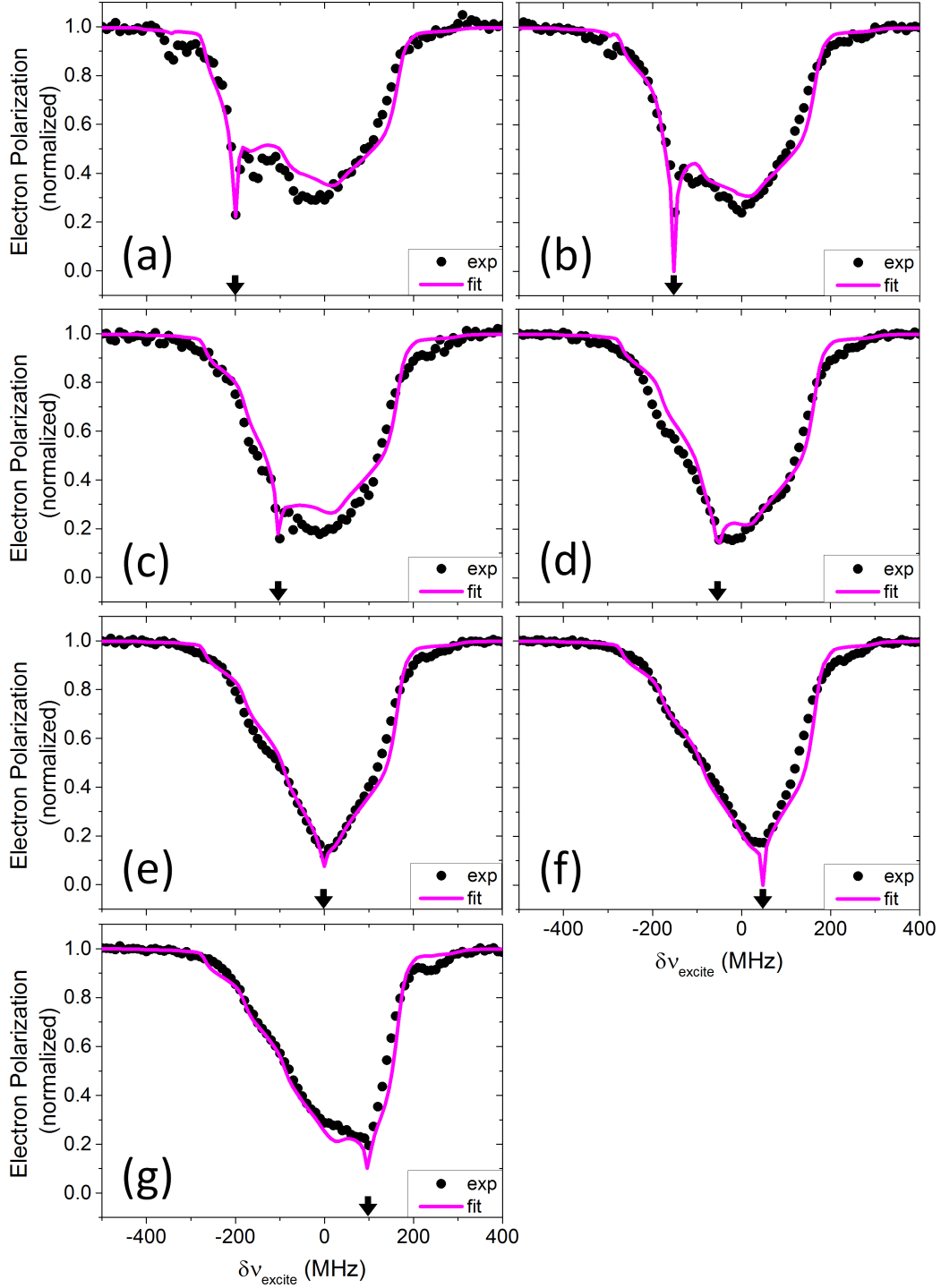


Figure. S3: Experimental ELDOR spectra measured at 20 K on the “H₂O” sample (black symbols) overlaid with the simulated ELDOR spectra (magenta lines). The detection frequencies are marked by the small black arrows: (a) $\delta\nu_{detect} = -200$ MHz, (b) $\delta\nu_{detect} = -150$ MHz, (c) $\delta\nu_{detect} = -100$ MHz, (d) $\delta\nu_{detect} = -50$ MHz, (e) $\delta\nu_{detect} = 0$ MHz, (f) $\delta\nu_{detect} = 50$ MHz and (g) $\delta\nu_{detect} = 100$ MHz. The x-axis is plotted with reference to $\nu_{ref} = 95$ GHz.

ELDOR spectra were not measured on the “D₂O” sample. However, we were able to fit the DNP spectra of the “D₂O” sample by simulating the electron polarization using the

same parameters used for the “H₂O” sample, and just decreasing the value of \bar{A}^\pm by a factor of two, in order to mimic the increased distance between the D₂O molecules and the radical molecule. The simulations appear in Figs. S4 and S5, and are discussed in the main text. The simulation parameters can be found in the main text as well. As can be seen from Fig. S6, the DNP fits are similar to the “H₂O” case (see main text), and all the same discrepancies can be found. In Fig. S7 we plot the quality of the ¹H-DNP fits as a function of Λ^{eSD} and \bar{A}^\pm for $T_{2e} = 10\mu s$ and $T_{2e} = 100\mu s$, and at 6K and 20K for the “D₂O” sample. From Fig. S7a it is evident that keeping the “H₂O” parameters and just decreasing the value of \bar{A}^\pm by a factor of two works well at 6K. However, looking at Fig. S7c shows that we do not get the best quality fit at 20K. Fig. S7b and d show that if we were to change the $T_{2e} = 100\mu s$ we would have had to change the fitting parameters, as was also shown in the “H₂O” case shown in the main text.

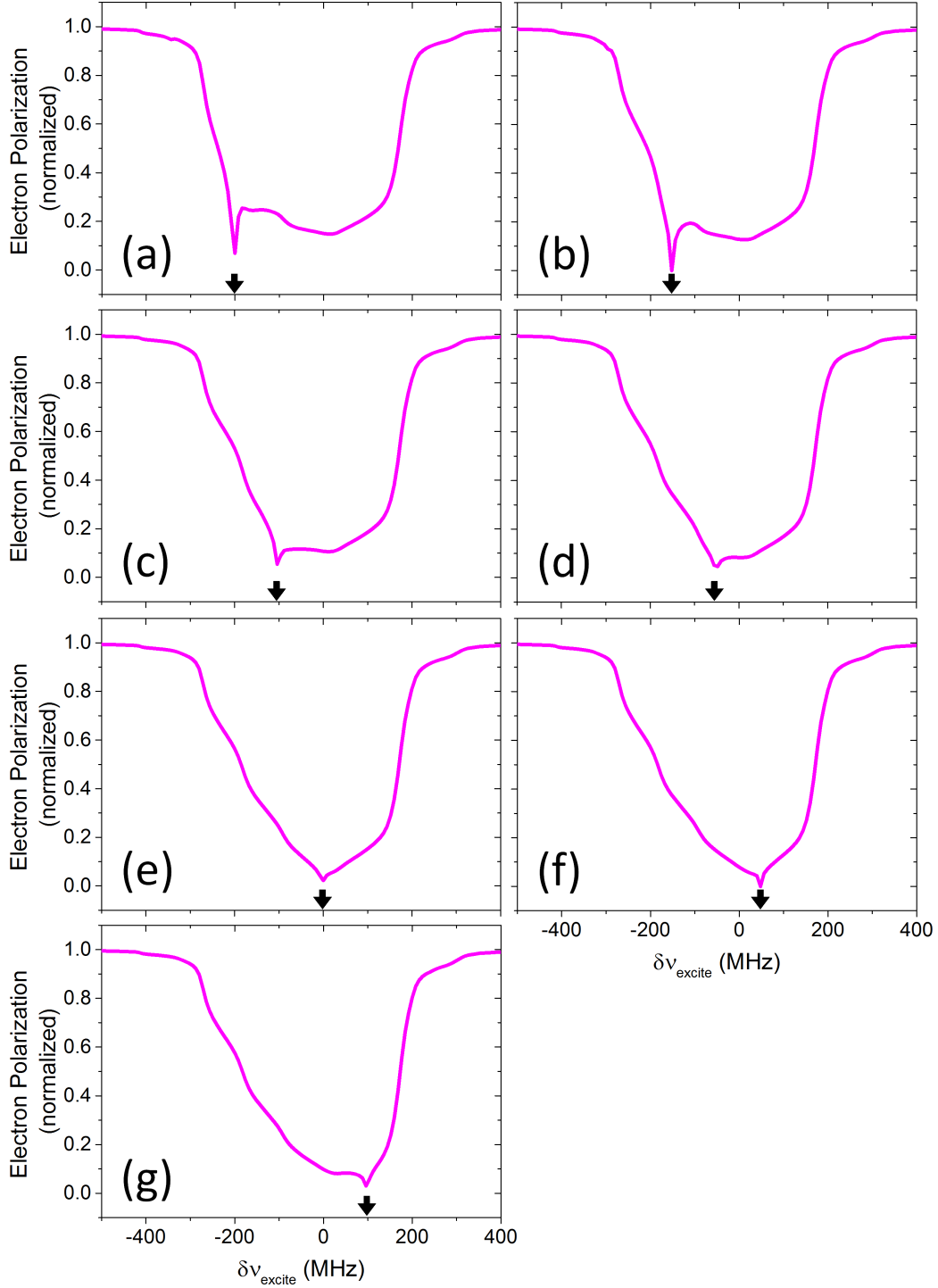


Figure. S4: Simulated ELDOR spectra for the “D₂O “ sample using the simulation parameters for the “H₂O” sample at 6 K, and halving the \bar{A}^{\pm} value. The detection frequencies are marked by the small black arrows: (a) $\delta\nu_{detect} = -200$ MHz, (b) $\delta\nu_{detect} = -150$ MHz, (c) $\delta\nu_{detect} = -100$ MHz, (d) $\delta\nu_{detect} = -50$ MHz, (e) $\delta\nu_{detect} = 0$ MHz, (f) $\delta\nu_{detect} = 50$ MHz and (g) $\delta\nu_{detect} = 100$ MHz. The parameters for the simulations are given in the main text. The x-axis is plotted with reference to $\nu_{ref} = 95$ GHz.

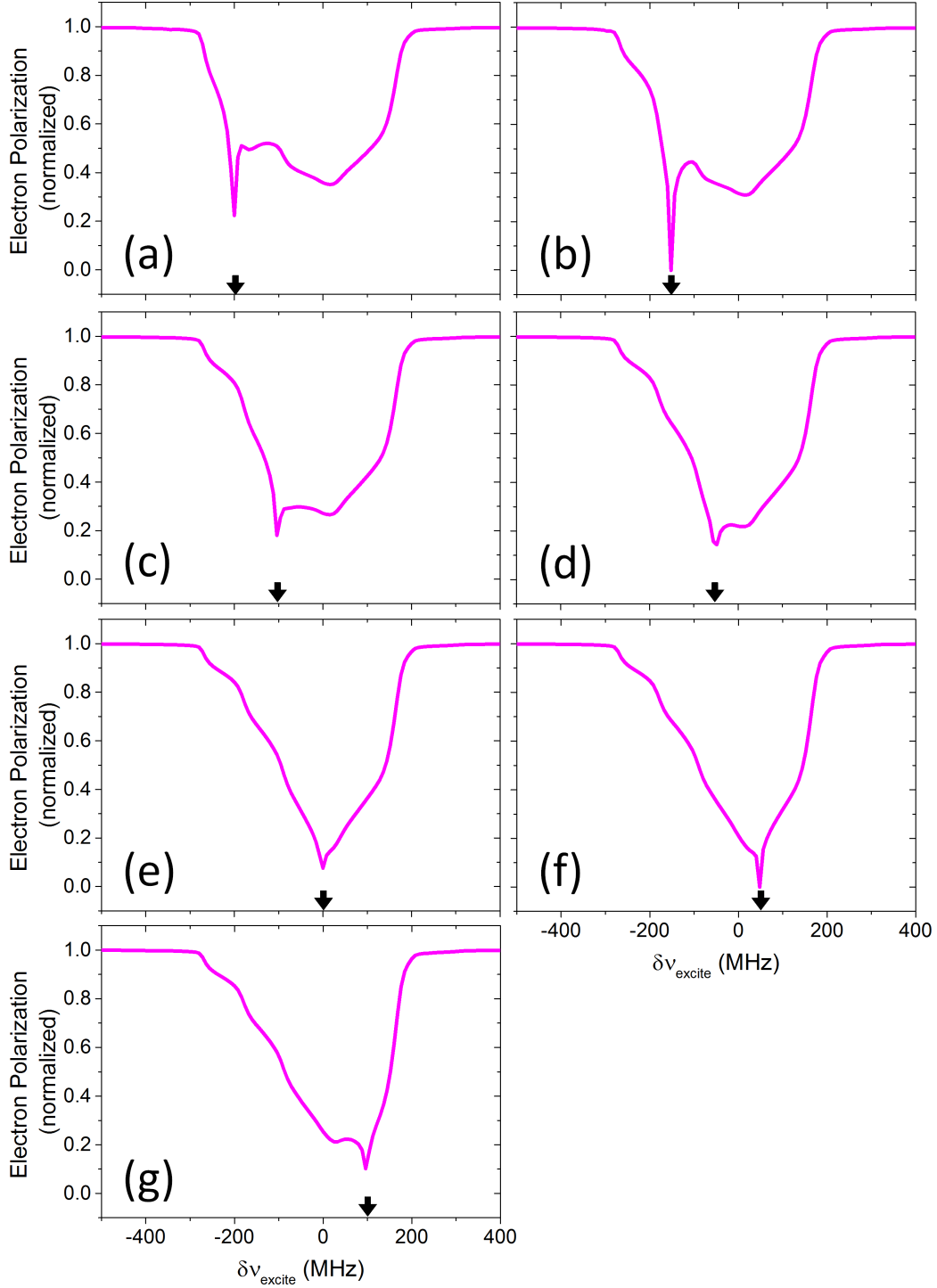


Figure. S5: Simulated ELDOR spectra for the “D₂O “ sample using the simulation parameters for the “H₂O” sample at 20 K, and halving the \bar{A}^{\pm} value. The detection frequencies are marked by the small black arrows: (a) $\delta\nu_{detect} = -200$ MHz, (b) $\delta\nu_{detect} = -150$ MHz, (c) $\delta\nu_{detect} = -100$ MHz, (d) $\delta\nu_{detect} = -50$ MHz, (e) $\delta\nu_{detect} = 0$ MHz, (f) $\delta\nu_{detect} = 50$ MHz and (g) $\delta\nu_{detect} = 100$ MHz. The parameters for the simulations are given in the main text. The x-axis is plotted with reference to $\nu_{ref} = 95$ GHz.

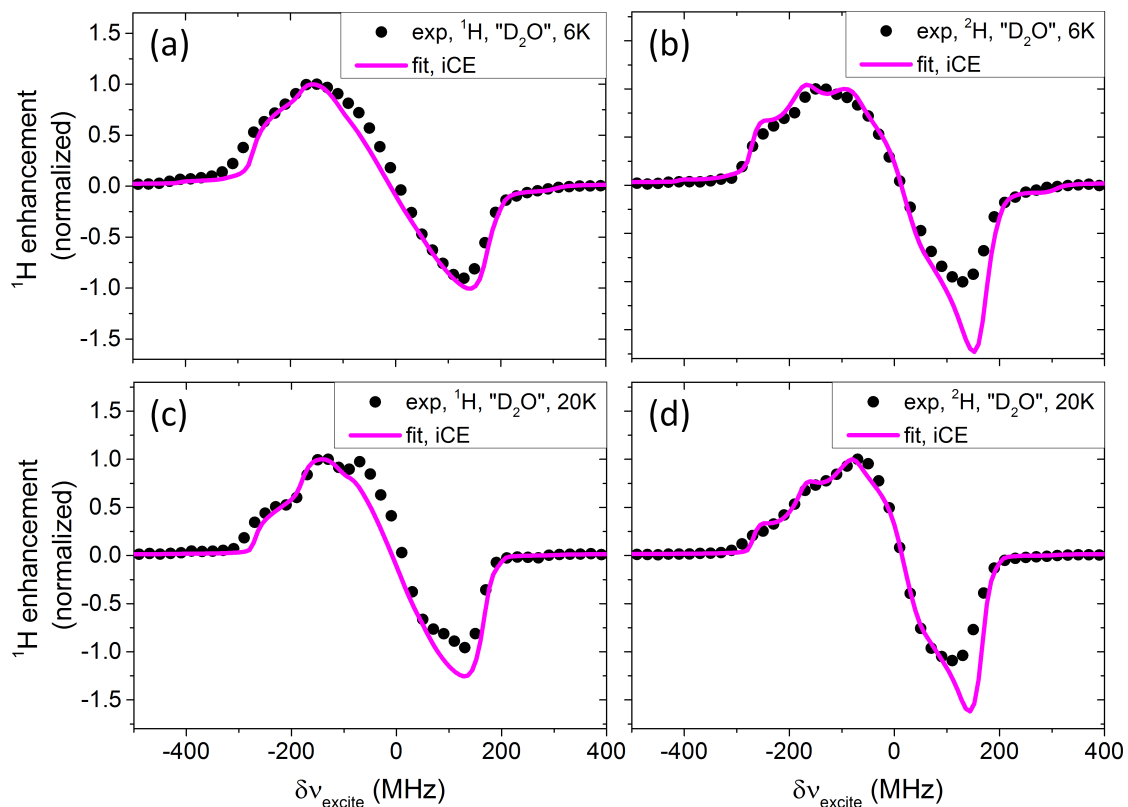


Figure. S6: Experimental ^1H -DNP spectra (a and c, black symbols) and ^2H -DNP spectra (b and d, black symbols) measured on the “ D_2O ” sample at (a-b) 6 K and (c-d) 20 K. The experimental spectra are overlaid with the simulated iCE-DNP spectra of the appropriate nucleus (magenta lines). The parameters for the simulations are given in the main text. The x-axis is plotted with reference to $\nu_{\text{ref}} = 95$ GHz.

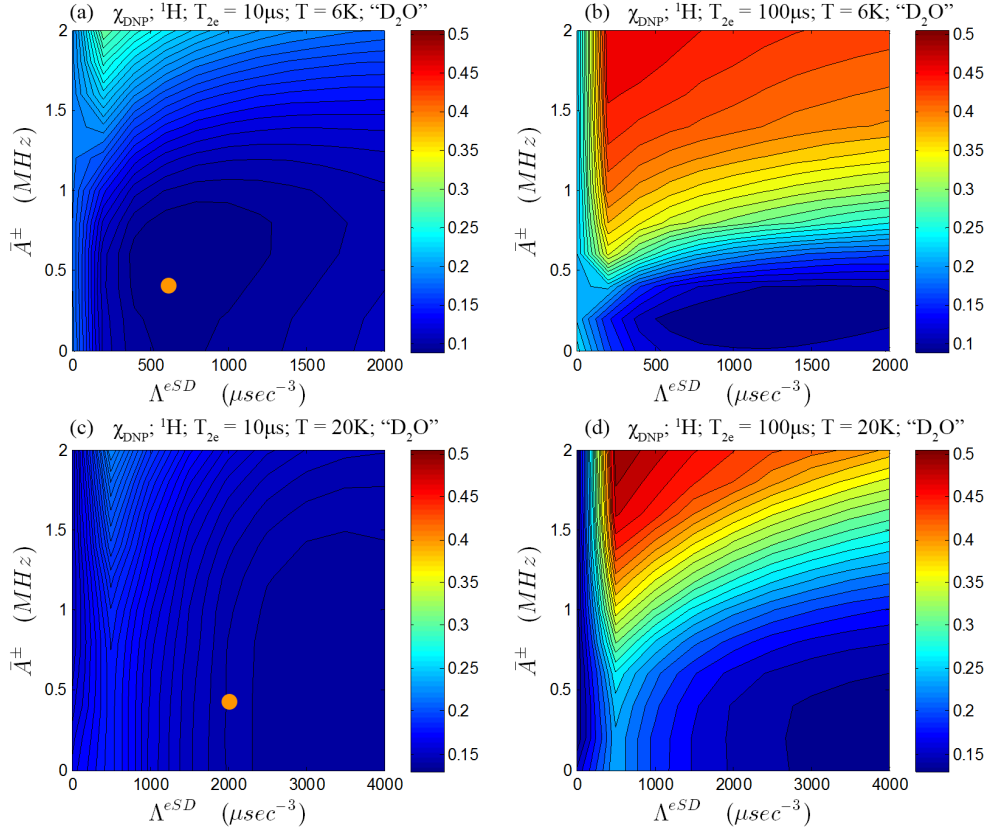


Figure. S7: Quality of fit to the ^1H -DNP spectrum measured at (a and b) 6K and (c and d) 20K for the “ D_2O ” sample, plotted against \bar{A}^\pm and Λ^{eSD} for (a and c) $T_{2e} = 10\mu\text{s}$ and (b and d) $T_{2e} = 100\mu\text{s}$. The orange dot marks the values of \bar{A}^\pm and, Λ^{eSD} and T_{2e} used for the final ELDOR analysis, as listed in Table 1 in the main text. The rest of the parameters used for simulations are listed in Table 1 in the main text as well.

Next we were able to fit the 40 K ^2H -DNP spectrum measured on the “ H_2O ” sample (see Fig. S8). The fit was done by simulating the electron polarization assuming the same parameters as at 20 K and just changing the T_{1e} value to the 40 K experimental value. The simulation parameters can be found in the figure caption. As can be seen, the fit is good and all the major features of the ^2H -DNP spectrum, especially the steps on the low frequency side. The discrepancy around +110 MHz that was seen in other ^2H spectra can also be found here, though it is smaller than in other cases.

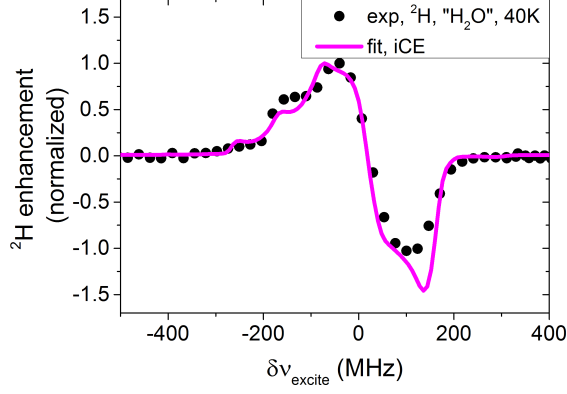


Figure. S8: Experimental ^2H -DNP spectrum measured on the “ H_2O ” sample at 40 K (black symbols) overlaid with the simulated ^2H -iCE-DNP spectrum (magenta lines). The parameters for the simulations are: $T_{1e} = 30$ msec (measured at 40 K), $T_{1H} = 13$ sec (measured at 20 K), $T_{2e} = 10$ μsec , $\overline{A}^\pm = 0.8$ MHz, $\Lambda^{eSD} = 2000$ μsec^{-3} and $T_{max}^{eSD} = 0.009$ msec. The x-axis is plotted with reference to $\nu_{ref} = 95$ GHz.

In the main text we describe the DNP recovery experiment where we polarize both ^1H and ^2H nuclei, then saturate the ^1H nuclei for a short time and then watch the ^1H enhancement partially recover. In this experiment three timescales were seen: a very fast reappearance of some ^1H polarization, then a slower rising component, and finally a decay of saturation back to the ^1H thermal equilibrium value. To verify this first fast timescale we conducted the same experiment on a “fully protonated” sample without deuterons. In this experiment the fast reappearance of some ^1H polarization happened with a time constant of 0.08 sec, which is similar to the 1.2 sec seen in the DNP recovery experiment. A comparison between the DNP recover and a T_{1n} experiment on a “fully protonated” sample are shown in Fig. S9.

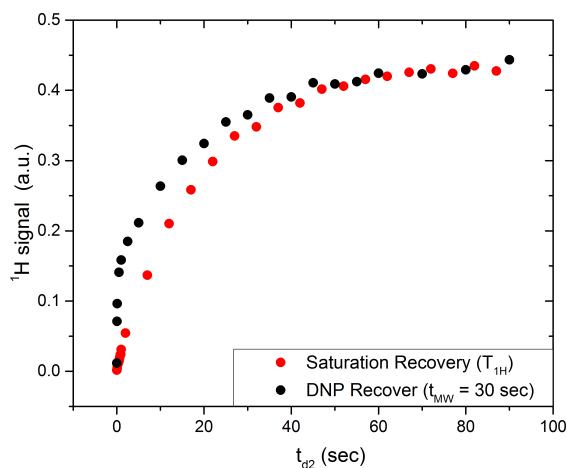


Figure. S9: Comparison of ^1H saturation recovery (black) and ^1H -DNP recovery (red) experiments on a “fully protonated” sample showing that during the DNP recover experiment (with $t_{excite} = 30$ sec) there is a very fast small recovery timescale and then the usual T_{1H} relaxation back to thermal equilibrium.

To further prove that the source of the ^2H recovered polarization lies in the ^1H pool we acquired the ^2H echo signal following a DNP period and a subsequent saturation of both ^1H and ^2H NMR signals (blue in Fig. S10). In this case the ^2H polarization hardly recovers, again confirming that the ^1H nuclei are the source of the recovered ^2H polarization in the above experiment. This is compared to the ^2H echo measured when do not apply saturation pulses on the ^1H nuclei (red in Fig. S10).

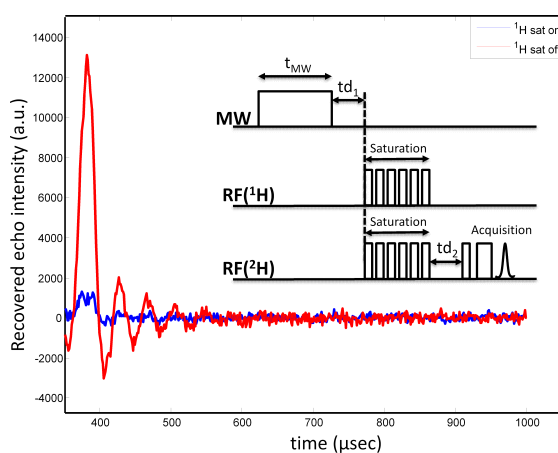


Figure. S10: Comparison of the ^2H echo signal during a ^2H -DNP recovery experiment with (blue) and without (red) additional saturation of the ^1H nuclei. When both the ^2H and ^1H nuclei are saturated the ^2H nuclei do not recover their polarization, but when only the ^2H nuclei are saturated, the ^2H nuclei can recover.

References

- [1] A. Feintuch, D. Shimon, Y. Hovav, D. Banerjee, I. Kaminker, Y. Lipkin, K. Zibzener, B. Epel, S. Vega and D. Goldfarb, *J. Magn. Reson.*, 2011, 209, 136-141